Evaluation of Silicon Diaphragms for Hermetic Packaging of Microbolometer Arrays

Xia, Hexin; Akram, Muhammad Nadeem; Bardalen, Eivind; Roy, Avisek; Aasmundtveit, Knut; Øhlckers, Per

Department of Microsystems University of South-Eastern Norway

Xia, H., Akram, M. N., Bardalen, E., Roy, A., Aasmundtveit, K. E., & Ohlckers, P. (2020, September 15-18). Evaluation of Silicon Diaphragms for Hermetic Packaging of Microbolometer Arrays. In K. Aasmundtveit, K. Imenes & P. M. Svasta (Eds.), *2020 IEEE 8th Electronics System-Integration Technology Conference (ESTC)* (pp. 1-5). IEEE. https://doi.org/10.1109/ESTC48849.2020.9229710

Publisher's version: DOI: 10.1109/ESTC48849.2020.9229710

© 2020 IEEE. Personal use of this material is permitted. Permission from IEEE must be obtained for all other uses, in any current or future media, including reprinting/republishing this material for advertising or promotional purposes, creating new collective works, for resale or redistribution to servers or lists, or reuse of any copyrighted component of this work in other works.

Evaluation of Silicon Diaphragms for Hermetic Packaging of Microbolometer Arrays

Hexin Xia
Department of Microsystems
University of South-Eastern Norway
Horten, Norway
Hexin.Xia@usn.no

Muhammed Nadeem Akram
Department of Microsystems
University of South-Eastern Norway
Horten, Norway
Muhammed.N.Akram@usn.no

Eivind Bardalen
Department of Microsystems
University of South-Eastern Norway
Horten, Norway
Eivind.Bardalen@usn.no

Avisek Roy
Department of Microsystems
University of South-Eastern Norway
Horten, Norway
Avisek.Roy@usn.no

Knut Eilif Aasmundtveit
Department of Microsystems
University of South-Eastern Norway
Horten, Norway
Knut.Aasmundtveit@usn.no

Per Ohlckers
Department of Microsystems
University of South-Eastern Norway
Horten, Norway
Per.Ohlckers@usn.no

***Abstract*— Hermetic packaging is a critical requirement for microbolometers to maintain long-term reliability. A thinner diaphragm is desirable for vacuum packaging of microbolometers to obtain higher infrared light transmission. However, a thinner diaphragm results in a larger deflection due to the pressure difference from atmosphere, which may influence the IR signal focus and possibly cause mechanical failure. In this paper, the trade-offs of using thin single crystal silicon diaphragms as encapsulation for hermetic packaging of microbolometer arrays have been investigated in terms of the mechanical stability and optical performance using COMSOL and Zemax. The optical simulations show that the bending of the thin diaphragm has negligible effect on the infrared light focus with wavelengths from 8 to 14 µm. The mechanical simulations reveal that a thin diaphragm (thickness < 70 µm) with 10×10 mm^2 area and a diaphragm (thickness < 90 µm) with 12×12 mm^2 area will cause mechanical failure, and the designed diaphragm thickness must incorporate margins to these values.**

Keywords—hermetic packaging, deflection, mechanical stability, IR sensor

I. Introduction

Infrared thermal imaging systems have broad prospects in both military and civilian fields. For example, security monitoring, night-time vehicle detection, and industrial process control [1]. Microbolometer arrays (MBAs) are the core detectors of uncooled infrared thermal cameras. Typical microbolometer-based infrared (IR) light cameras consist of three elements: an optical lens, the microbolometer sensor and back-end electronics [2]. The system configuration is illustrated in Fig. 1. A lens is used to bring the IR light to a fixed focal point on the microbolometer sensors. When the longwave IR (LWIR) light with 8-14 µm wavelength strikes the sensing pixel array, the electrical resistivity of the materials change due to heating. The acquired change in resistivity is converted to electrical information and then transferred to the read-out integrated circuit (ROIC). The ROIC sends the data to the output for further image processing [2].

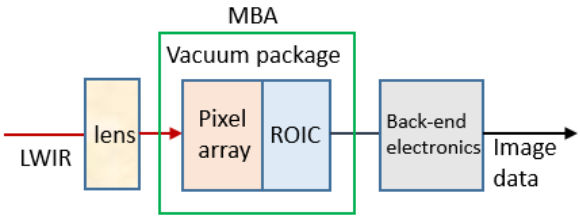

Fig. 1. Simple system configuration illustration of a typical microbolometer based IR camera.

In order to ensure necessary performance, the MBAs are encapsulated inside a vacuum atmosphere with a vacuum level lower than 10^{-4} mbar [3]. Several microelectromechanical systems (MEMS) devices, such as resonators and internal sensors rely on operation in vacuum to obtain the required specifications [3]. The packaging approach applied for encapsulating a MEMS device with hermetic seals in a vacuum environment is referred to as hermetic packaging [4].

Typically, the vacuum is maintained by bonding a micromachined diaphragm to the device, as illustrated in Fig. 2, where MBAs are fabricated on top of ROICs. The diaphragm needs to be transparent to the LWIR light [5]. A thinner diaphragm is desirable for higher IR transmission and for obtaining larger cavity volume to maintain high vacuum [6]. Thin diaphragms (< 300 µm) made by optically transparent materials is able to provide the low loss transmission of IR, which is critical for the operation of MBAs [7]. Diaphragms with a thickness lower than 100 µm can also be useful for the applications of measuring the vacuum level inside hermetic packages as a larger diaphragm deflection will provide better pressure sensitivity [8, 9]. The diaphragm covering the vacuum cavity will deflect due to the pressure difference between the surrounding atmosphere and the low-pressure atmosphere inside packaging, as seen Fig. 3. A thinner diaphragm gives larger deflection, which may influence the IR transmission and thus affect the performance of MBAs. If the thickness of the diaphragm is too thin, fracture may occur when the stress on the thinner diaphragm exceeds the fracture strength.

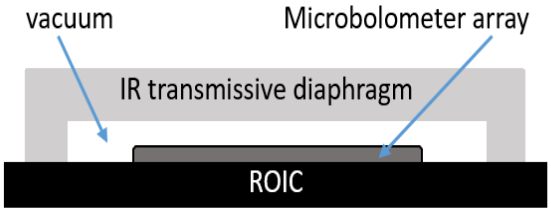

Fig. 2. Hermetic packaging of microbolometer array.

In this paper, the trade-offs of thinner diaphragms are discussed. This study provide insights into the mechanical and optical effect of thin diaphragms in MBAs packaging and benefit the further research of hermetic packaging for MEMS devices.

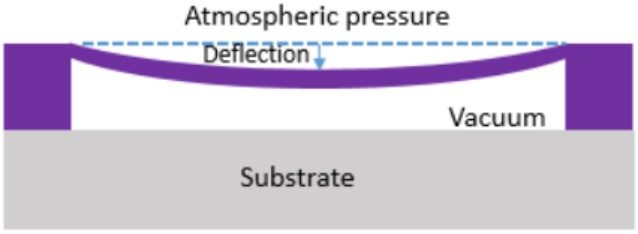

Fig. 3. Deflection of the hermetically sealed diaphragm under differential pressure.

II. Modelling and Methodology

The finite element (FE) method was applied using COMSOL Multiphysics for detecting the maximum allowed deformation and stress of the thin diaphragm. Ray tracing software Zemax was used for assessing the effect of a deformed diaphragm on the IR transmission. The deflection of the diaphragm is based on the deformation results obtained from COMSOL simulations.

A. Deformed Diaphragms

An analytical expression for the relationship between pressure and displacement for square diaphragms is presented in (1) [10].

$$w(x,y) = 0.0213p\frac{a^4}{D}\left(1-\frac{x^2}{a^2}\right)^2\left(1-\frac{y^2}{a^2}\right)^2 \quad (1)$$

where p is pressure, a represents half side length of the square diaphragm, and x and y are the coordinates of the geometries. The value of maximum displacement of the diaphragms is located at center of the diaphragms (x=0, y=0). The maximum displacement can be estimated by (2).

$$w(0,0) = \frac{pa^4}{64D} \quad (2)$$

D is defined as the flexure rigidity of the diaphragm:

$$D = \frac{Eh^3}{12(1-\nu^2)} \quad (3)$$

where h represents the varied thickness of the diaphragms. E is Young's modulus and ν is Poisson's ratio. E and ν are material dependent parameters.

B. Finte Element Model Description

The analytical expressions can only provide an approximate displacement value. Numerical analysis such as FE method is the only way to achieve accurately values of the displacement.

A 3D model of a square diaphragm was built in COMSOL Multiphysics, where the cavity was set to a high vacuum (10^{-6} mbar) for intended simulations. The outer pressure p was atmospheric pressure (1 atm). The thickness of the diaphragm was varied in the range of 60-300 µm. These simulations have been repeated for different diaphragm surface areas (8×8 mm^2, 10×10 mm^2 and 12×12 mm^2), varying around a typical MEMS device area of ~100 mm^2 to demonstrate various chip scale hermetic packages. Single crystal silicon (SCS) with crystal direction [100] was selected as the diaphragm material since it is transparent to IR light. It has a Young's modulus (E) of 130.3 GPa and Poisson's ratio (ν) of 0.278 [11].

In order to obtain accurate finite element analysis (FEA) results, it is important to select appropriate mesh settings. Fig. 4 shows the convergence of deflection as function of mesh density. Our simple geometry and short operation time of the simulations allowed selecting a mesh density significantly higher than the minimum needed for convergence.

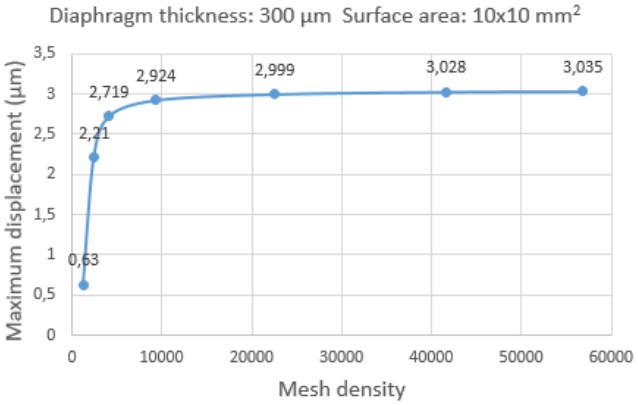

Fig. 4. Maximum displacement at different mesh density when diaphragm thickness is 300 µm and surface area is 10x10 mm^2.

C. Optical Simulations Description

A lens is required to focus the IR light on the image sensor. The F-number of the lens (equation 4) is crucial for determining the performance of the thermal imaging system. F is the F-number, f is the focal length, which is the distance from lens to MBA sensor, and D_{EP} is the diameter of the aperture.

$$F = \frac{f}{D_{EP}} \quad (4)$$

In a typical IR lens, the F-number is equal to 1, which gives high contrast and satisfactory signal for objects in uncooled LWIR thermal cameras. Therefore, we decided to use a lens with a F-number equal to 1, where both the aperture diameter and focal length was set to 10 mm. The object distance is set to infinity. The main lens is set as an ideal paraxial lens, meaning that any light passing through it is focused on a single point.

III. Simulation Results

A. Deflection and Mechanical Stability

Fig. 5 shows the COMSOL simulation results with diaphragm thicknesses varied from 60 µm to 300 µm and with diaphragm surface area of 8×8 mm^2, 10×10 mm^2, and 12×12 mm^2 under the differential pressure load of 1 atm. Fig. 5(a) shows the maximum displacement and Fig. 5(b) shows the maximum first principle stress. From Fig. 5(a) the deflection increases with an increase in surface area of the cavity, and the difference is more pronounced as the cap thickness decreases. The maximum displacement and associated stress of the diaphragms start to saturate for diaphragm thickness values higher than 200 µm.

Fig. 6 presents the top view of first principal stress distribution and cross-sectional view with a surface area of 10×10 mm^2 at a diaphragm thickness of 200 µm and 60 µm. There is no change in first principle stress distribution when changing the thickness of the diaphragm, as evident from Fig. 6(a) and (c). Fig. 6(b) and (d) shows that the maximum stress is concentrated at the edges of the silicon diaphragm. When the thickness of the silicon diaphragm with surface area of 10x10 mm^2 decreases from 200 µm to 60 µm, a noticeable deflection due to pressure difference is observed (Fig. 6(d)).

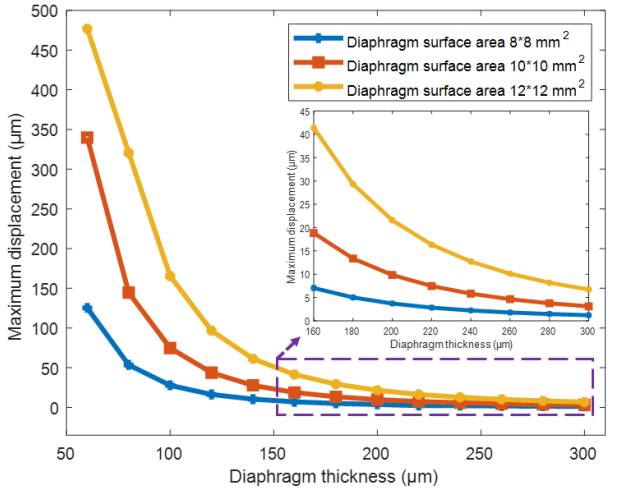

(a)

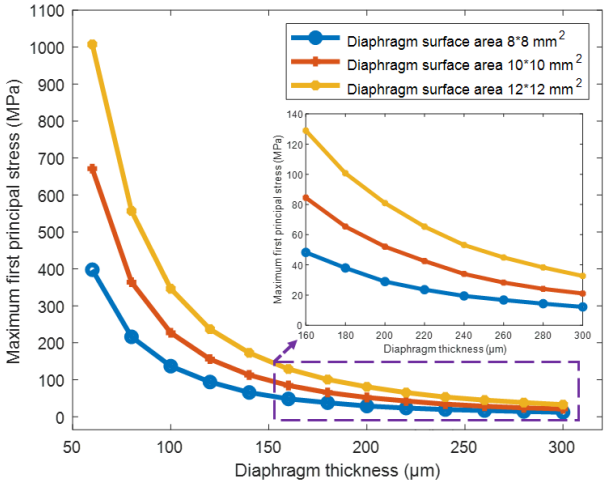

(b)

Fig. 5. (a) Maximum displacement and (b) Maximum first principle stress of a silicon diaphragm with different surface areas (8×8 mm^2, 10×10 mm^2 and 12×12 mm^2) as a function of diaphragm thickness at a differential pressure of 1 atm.

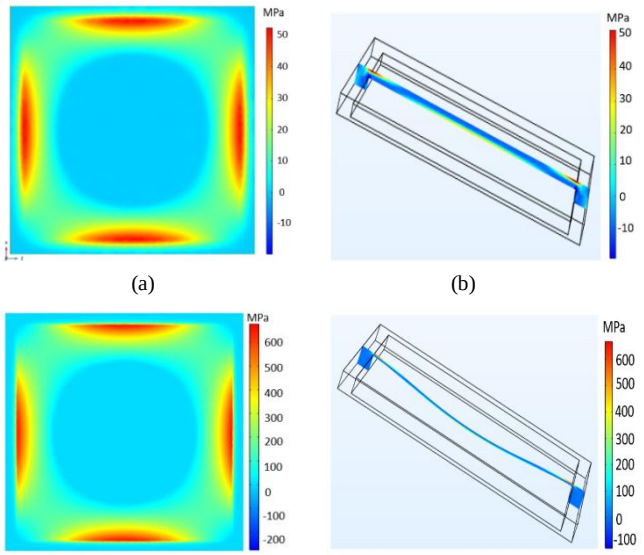

(a) (b)

(c) (d)

Fig. 6. First principle stress distribution for a surface area of 10×10 mm^2 with 200 μm thickness. (a) Top and (b) cross-sectional view. With 60 μm thickness. (c) Top and (d) cross-sectional view.

B. *Optical Perfromance*

Fig. 7 shows the layout of the optical design. The wavelength is set to 10 μm as mentioned above. The four field angles: 0°, 10°, 20°, and 30° are selected and marked with blue, green, red and yellow color, respectively. The initially flat 70 μm thin silicon diaphragm has an undistorted distance of 300 μm to the microbolometer image sensor. For simplicity of the simulation, a radius of curvature of 47 mm is applied to the diaphragm. This is taken from the maximum displacement of 213 μm at the center of the 70 μm diaphragm with 10x10 mm^2 area obtained from COMSOL simulations. In other words, the diaphragm was bent and consequently reduced the distance between the diaphragm and the microbolometer to 253 μm.

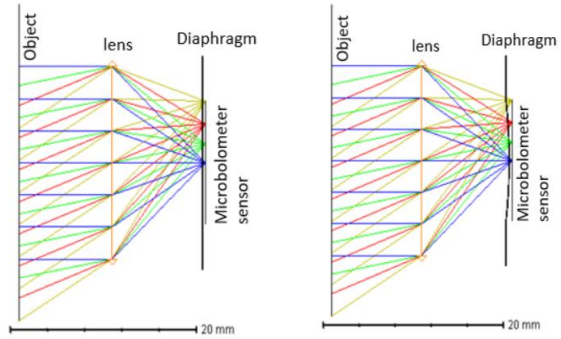

(a) (b)

Fig. 7. Layout of optical design with a 10 μm wavelength and four incident angles 0°, 10°, 20°, and 30°. Diaphragm thickness is 70 μm. (a) before and (b) after bending.

Ray spot diagrams and the modulation transfer functions (MTF) was calculated in Zemax to evaluate the image quality resulting from the transmitted IR light through the bent diaphragm. The ray spot diagram gives indication of the image quality of a point object. In the absence of aberrations, a point object will converge to a perfect image point. Fig. 8 shows the image surface (IMA) spot diagram of the diaphragm before (a) and after (b) deflection. Object (OBJ) describes the location of the field points in terms of field angles: 0°, 10°, 20°, and 30° at a wavelength of 10 μm. The black circles are Airy discs, which when enclosing all the rays indicates that the system is diffraction limited. Moreover, the location of the centroid on the imaging surface where the IR light will focus is given by the IMA. As seen in the Fig. 8, after bending the IMA slightly change from 1.764 mm, 3.641 mm, and 5.774 mm to 1.766 mm, 3.644 mm and 5.780 mm under incident angles 10°, 20°, and 30°, whereas the IMA at the center remain unchanged. For all angles the IMA is still within the Airy disc, indicating that the performance is diffraction limited.

The simulated Modulation Transfer Function (MTF) is a plot of modulation versus spatial frequency. The spatial frequency gives an indication of the image resolution and the modulation give an indication of the image contrast. Hence, MTF is able to quantify the overall imaging performance of a system in terms of resolution and contrast. Fig. 9 shows MTF with different incident angles before (a) and after deflection (b) of the diaphragm, where T is tangential MTF curve and S is sagittal MTF curve at the specified field point, where the field points are specified in terms of the field angles. There is virtually no drop of MTF after bending.

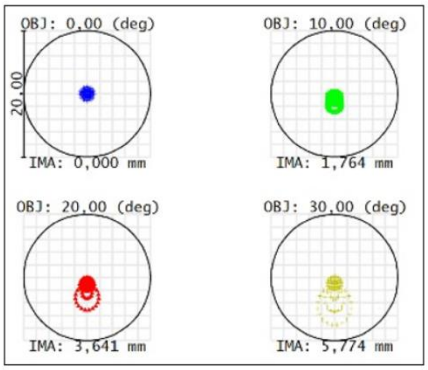

(a)

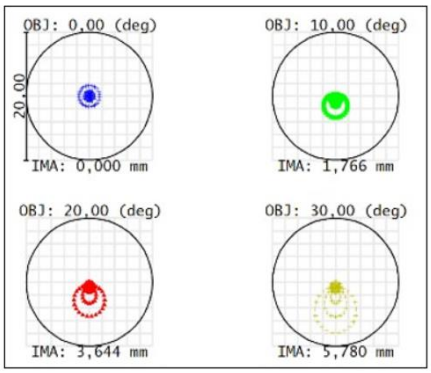

(b)

Fig. 8. Ray spot diagram with diaphragm thickness 70 µm and surface area 10×10 mm^2. (a) before and (b) after deflection.

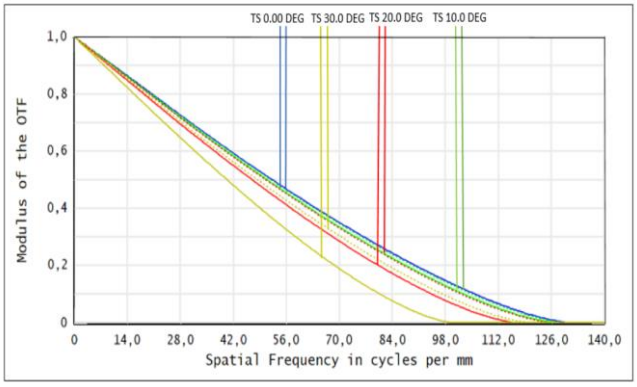

(a)

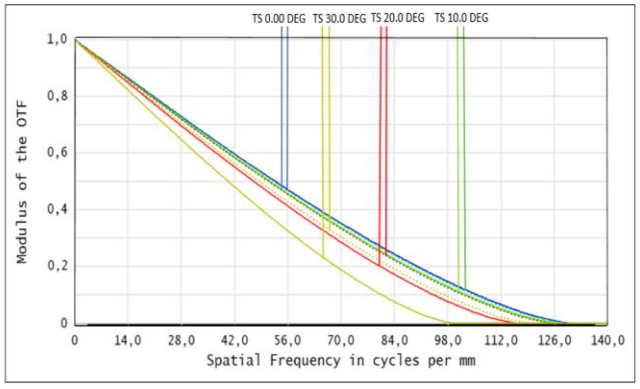

(b)

Fig. 9. MTF curves with diaphragm thickness 70 µm and surface area 10×10 mm^2 before (a) and after (b) deflection. T is tangential MTF curve and S is sagittal MTF curve at the specified field point.

IV. Disscussion

We have considered the minimum diaphragm thickness assuming a fracture strength around 500 MPa [12], and found the minimum diaphragm thickness to be 70 µm and 90 µm for a surface area of 10×10 mm^2 and 12×12 mm^2, respectively. For a smaller surface area of 8×8 mm^2 we did not observe failure in the range of 60-300 µm diaphragm thickness, meaning that the diaphragm can likely be even thinner than 60 µm for this surface area. Thin diaphragms are beneficial for minimizing optical absorption. They also give larger deflection due to the differential pressure to enable more accurate measurements of the hermeticity of the package. The diaphragm thickness should be designed with a considerable margin to the minimum allowed thickness, to allow for process variations for instance in the etching step of the diaphragm wafer.

Stresses induced by bonding can cause a slight deflection in the diaphragm even in the absence of a pressure gradient. In the case of wafer-level packaging (WLP) the dicing will occur after packaging and could potentially cause diaphragm failure if the diaphragm is too thin. Even thicker diaphragms can be considered since IR light have low optical loss within 300 µm [7]. This will, however, give a lower cavity volume being more sensitive to vacuum deterioration compared with a higher cavity volume and equal leak rate. These considerations are beyond the scope of this study. Based on the simulation results in Fig. 5, a diaphragm thickness of 100 µm at surface area 8×8 mm^2 , 150 µm at 10×10 mm^2 and 200 µm at 12×12 mm^2 seem to be a good recommendation.

In terms of optical performance, IMA only change about 0.1% when the diaphragm deflects. The contrast and resolution are not affected, as evidenced by the MTF curves. The bending has negligible effect on the IR light propagation and will therefore not influence the device performance. Our study shows that the microbolometer performance will not be affected by the diaphragm thickness in the range of 60-300 µm. It should be noted that the simulations are performed in an ideal setting with a perfect surface (paraxial lens) and does not consider properties such as surface roughness of the diaphragm due to etching, which could result in a considerable loss of IR signal.

V. Conclusion

In this paper, we have investigated SCS diaphragms for encapsulation in hermetic packaging of microbolometer arrays. We found that a SCS diaphragm with a surface area of 10×10 mm^2 should have a thickness above 70 µm and for a 12×12 mm^2 surface area the diaphragm should be thicker than 90 µm to prevent mechanical failure. The LWIR light is relatively (0.1%) unaffected by the bending of the diaphragm resulting from the differential pressure. Taking practical considerations into account, we suggest that the diaphragm should be above 100 µm for a 8×8 mm^2 area, 150 µm for a surface area of 10×10 mm^2 and 200 µm for an area of 12×12 mm^2.

Acknowledgment

This work was carried out with funding by the ECSEL Joint Undertaking (JU) project APPLAUSE under grant agreement No 826588. The JU receives support from the European Union's Horizon 2020 research and innovation programme. The Research Council of Norway is also acknowledged for the

support to APPLAUSE and the Norwegian Micro- and Nano-Fabrication Facility (NorFab, project number: 245963/F50).

REFERENCES

[1] Becker, L., Influence of IR sensor technology on the military and civil defense. Integrated Optoelectronic Devices 2006. Vol. 6127. 2006: SPIE.

[2] Ostrower, D., Optical Thermal Imaging – replacing microbolometer technology and achieving universal deployment. III-Vs Review, 2006. 19(6): p. 24-27.

[3] Kang, S.J., et al., Vacuum-controlled wafer-level packaging for micromechanical devices. Japanese Journal of Applied Physics, 2014. 53(6): p. 066501.

[4] Lee, S.-H., et al., Wafer-level vacuum/hermetic packaging technologies for MEMS. SPIE MOEMS-MEMS. Vol. 7592. 2010: SPIE.

[5] Hilton, A., et al., WAFER-LEVEL VACUUM PACKAGING OF MICROBOLOMETER-BASED INFRARED IMAGERS. 2016.

[6] Wiel, H.J.v.d., et al. Systematic characterization of key parameters of hermetic wafer-level Cu-Sn SLID bonding. in 2013 Eurpoean Microelectronics Packaging Conference (EMPC). 2013.

[7] Wang, X., et al., Wafer-Level Vacuum Sealing by Transfer Bonding of Silicon Caps for Small Footprint and Ultra-Thin MEMS Packages. Journal of Microelectromechanical Systems, 2019. 28(3): p. 460-471.

[8] Lellouchi, D., et al., A new method for the hermeticity testing of wafer-level packaging. Journal of Micromechanics and Microengineering, 2010. 20(2): p. 025031.

[9] Pham, N.P., et al. Metal-bonded, hermetic 0-level package for MEMS. in 2010 12th Electronics Packaging Technology Conference. 2010.

[10] Bao, M.-H., Chapter 2 - Basic mechanics of beam and diaphragm structures, in Handbook of Sensors and Actuators, M.-H. Bao, Editor. 2000, Elsevier Science B.V. p. 23-88.

[11] Cho, C.-H., Characterization of Young's modulus of silicon versus temperature using a "beam deflection" method with a four-point bending fixture. Current Applied Physics - CURR APPL PHYS, 2009. 9: p. 538-545.

[12] Steiert, M. and J. Wilde, Influence of dicing damages on the thermo-mechanical reliability of bare-chip assemblies. Microelectronics Reliability, 2014. 54(9): p. 1686-1691.